



# Effect of phase on the frictional dissipation in systems subjected to harmonically varying loads

Yong Hoon Jang<sup>a,\*</sup>, J.R. Barber<sup>b</sup>

<sup>a</sup> School of Mechanical Engineering, Yonsei University, 50 Yonsei-ro, Seodaemun-gu, Seoul 120-749, Republic of Korea

<sup>b</sup> Department of Mechanical Engineering, University of Michigan, Ann Arbor, MI 48109-2125, USA

## ARTICLE INFO

### Article history:

Received 8 December 2010

Accepted 27 January 2011

### Keywords:

Contact problems

Fretting

Coulomb friction

Hysteretic damping

## ABSTRACT

When contacting elastic systems are subjected to periodic loading, frictional slip occurs resulting in energy dissipation. Here we investigate the effect of the relative phase of harmonically varying tangential and normal loads on the frictional dissipation in a very simple uncoupled frictional system. We demonstrate that this effect is substantial when the system experiences periods of separation, but more modest when contact is continuous. The maximum dissipation occurs when the normal and tangential loads are approximately  $\pi/2$  out of phase.

© 2011 Elsevier Masson SAS. All rights reserved.

## 1. Introduction

If two contacting elastic bodies are subjected to a combination of normal and tangential loads below the threshold needed to produce sliding, the contact area will usually comprise regions of ‘stick’ where there is no relative motion, and of ‘microslip’ where slip displacements are resisted by frictional tractions. A simple problem of this kind is the Hertzian contact between two large bodies with quadratic surfaces. Cattaneo (1938) and later Mindlin (1949) considered the case where such a contact is loaded first by a normal load  $P$  and then by a monotonically increasing tangential load  $Q$ , leading to an annulus of microslip that grows at the expense of the central stick region as the tangential load is increased. More general loading scenarios where both normal and tangential loading vary simultaneously were considered by Mindlin and Deresiewicz (1953). In particular, they showed that the entire contact area would remain in a state of stick as long as the normal load (and hence the size of the contact area) is increasing and  $d|Q|/dP < f$ , where  $f$  is the coefficient of friction. More recently, Ciavarella (1998) and Jäger (1998) extended Cattaneo’s solution method to describe any frictional elastic contact problem for which the two contacting bodies can be approximated as half spaces.

A problem of particular interest is that in which the applied loads are periodic in time, since numerous practical engineering systems are subject to vibration or repetitive loads and the microslip resulting at the contact interfaces causes energy

dissipation and hence influences the effective damping of the dynamic system. Furthermore, the inelastic processes associated with friction cause wear and can result in the initiation of fretting fatigue cracks that subsequently propagate under the influence of the periodic loads (Nowell et al., 2006). It seems reasonable to expect the rate of frictional energy dissipation to correlate with this type of damage.

Many periodic loading cycles might be described by the equations,

$$P(t) = P_0 + P_1 \sin(\omega t); \quad Q(t) = Q_0 + Q_1 \sin(\omega t + \phi), \quad (1)$$

where  $P_0, Q_0, P_1, Q_1$  are constants,  $\omega$  is a frequency,  $\phi$  is a phase angle and  $t$  is time. Notice that with a suitable datum for  $t$  and a suitable coordinate system, we can choose  $P_1, Q_1 \geq 0$  and restrict  $\phi$  to the range  $0 \leq \phi < \pi$  without loss of generality. This loading scenario plots out as an ellipse in  $PQ$ -space, as shown in Fig. 1.

The shape of the ellipse is defined by the phase angle  $\phi$ . The trajectory will be circular if  $P_1 = Q_1$  and  $\phi = \pi/2$  and it will reduce to a straight line if  $\phi = 0$ . The latter case is of some interest, since there will then be no dissipation in the Hertzian problem for any  $P_1, Q_1$  if  $Q_1 < fP_1$ . In this case, it is clear that the loading phase  $dP/dt > 0$  will satisfy Mindlin and Deresiewicz’ criterion for full stick, but the unloading phase passes through the same sequence of loading states as the loading phase and hence there is also no tendency for slip on unloading. However, if we now change the phase  $\phi$  from this limiting condition so as to generate an ellipse in Fig. 1, it is clear that some microslip is inevitable at least during the period that  $P$  is decreasing. This suggests that the phase of the loading has a major influence on dissipation and hence on the dynamics of the system.

\* Corresponding author. Tel.: +82 2 2123 5812; fax: +82 2 312 2159.

E-mail address: [yjh@yonsei.ac.kr](mailto:yjh@yonsei.ac.kr) (Y.H. Jang).

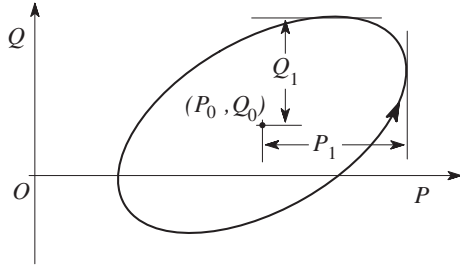


Fig. 1. Periodic loading scenario.

So far as the present authors are aware, no previous studies have remarked on this effect nor quantified its magnitude. In this paper, we shall therefore explore the effect of phase on frictional dissipation in the simplest possible contact system comprising a single elastically supported contact node with two degrees of freedom. This is in fact the same model that was previously used by Klarbring (1990) to elucidate the anomalies associated with large coefficients of friction in the discrete (e.g. finite element) solution of contact problems. Notably, he showed that there exists a critical coefficient of friction above which the frictional evolution problem is ill-posed in that there may exist either no solution or multiple solutions for a given loading scenario. Even below this critical coefficient of friction, the steady-state periodic behavior of a frictional elastic system can depend on the initial conditions. For example, Klarbring et al. (2007) have shown that a frictional ‘Melan’s theorem’ (i.e. that the system will always shakedown to a state involving no further slip, if such a state exists) if and only if the system is ‘uncoupled’, meaning that the normal reactions are independent of the tangential displacements. In all other (i.e. coupled) cases, scenarios can be devised in which the occurrence of shakedown depends on the initial conditions. It has been conjectured (Barber, under review) that this result is a special case of a more general principle that the frictional dissipation during periodic loading can depend on initial conditions if and only if the system is coupled, but no proof of this result is so far available.

In the present paper, we shall restrict attention to the uncoupled case, since our emphasis here is on the effect of phase on dissipation and it seems appropriate to examine this in the simplest possible context. We also remark that this condition is satisfied in many practical systems, including the Hertzian contact problem studied by Cattaneo (1938) and indeed any system in which the frictional contact occurs on a plane of symmetry.

## 2. The single-node system

The system to be analyzed is shown in Fig. 2(a) and comprises a rigid body supported by horizontal and vertical springs of stiffnesses  $k_{11}$ ,  $k_{22}$  respectively and making frictional contact with a horizontal rigid surface. Forces  $P(t)$ ,  $Q(t)$  are applied to the body causing horizontal and vertical displacements  $v$ ,  $\omega$  respectively. During contact, normal and frictional reactions  $N$ ,  $F$  respectively are induced at the interface.

We assume that the load changes sufficiently slowly for quasi-static conditions to apply, so that the body passes through a set of equilibrium states. We therefore obtain the two equilibrium equations

$$\begin{Bmatrix} F \\ N \end{Bmatrix} = \begin{Bmatrix} Q \\ P \end{Bmatrix} + \begin{bmatrix} k_{11} & 0 \\ 0 & k_{22} \end{bmatrix} \begin{Bmatrix} v \\ \omega \end{Bmatrix}, \quad (2)$$

where the sign conventions for  $N$ ,  $F$ ,  $v$ ,  $\omega$  are shown in Fig. 2(b). Notice that the off-diagonal terms in the stiffness matrix are zero because of the assumption that the system is uncoupled.

We assume that the evolution of the system is governed by the Coulomb friction law, which for this system requires that at any given time, the system be in one of four states defined as

$$\left. \begin{array}{l} \text{Stick} \quad \omega = 0; \quad \dot{v} = 0; \quad N \geq 0; \quad |F| \leq fN \\ \text{Separation} \quad \omega > 0; \quad N = 0; \quad F = 0 \\ \text{Forward slip} \quad \omega = 0; \quad \dot{v} > 0; \quad N \geq 0; \quad F = -fN \\ \text{Backward slip} \quad \omega = 0; \quad \dot{v} < 0; \quad N \geq 0; \quad F = fN \end{array} \right\}, \quad (3)$$

where the dot denotes the derivative with respect to time  $t$ . Once the reactions and displacements have been determined from conditions (1, 2, 3), the rate of frictional energy dissipation is defined by,

$$\dot{W} = -F(t)\dot{v}(t), \quad (4)$$

and the total energy dissipation per cycle can be obtained by integrating this expression around one complete cycle — i.e.

$$W = - \oint F(t)\dot{v}(t)dt. \quad (5)$$

Notice that the dissipation is always positive, since during slip the friction force always opposes the motion.

### 2.1. Normalization

The number of independent parameters in the problem can be reduced by an appropriate normalization. For this purpose, we define the dimensionless quantities

$$\hat{P} = \frac{P}{P_0}, \quad \hat{Q} = \frac{Q}{fP_0}, \quad \hat{N} = \frac{N}{P_0}, \quad \hat{F} = \frac{F}{fP_0}, \quad \hat{v} = \frac{k_{11}v}{Q_1}, \quad \hat{W} = \frac{k_{11}W}{fP_0Q_1}, \quad (6)$$

where the quantities  $P_0$ ,  $Q_0$  are defined through Eq. (1) and Fig. 1. Since the system is uncoupled and the steady state is unique, the only effect of the constant  $Q_0$  is to move the datum for tangential displacement by a constant  $Q_0/k_{11}$ , which has no effect on the dissipation  $W$ . We can therefore set  $Q_0 = 0$  without loss of generality.

We restrict attention to the case where the body would be in contact in the absence of vibration, so that  $P_0 > 0$ . In this case, the steady-state cycle will involve periods of separation if and only if  $P_1 > P_0$  and hence  $\hat{P}_1 > 1$ . Notice that no dissipation occurs during the separation phase and hence we do not need to normalize  $\omega$ . As a consequence, the stiffness  $k_{22}$  of the normal spring has no effect on the frictional energy dissipation.

Using these definitions, the dissipation per cycle takes the form,

$$\hat{W} = - \oint \hat{F}\hat{v}dt, \quad (7)$$

where  $\hat{F}$ ,  $\hat{v}$  can be obtained from the reduced set of conditions

$$\left. \begin{array}{l} \text{Stick} \quad \hat{v} = 0; \quad \hat{P} \geq 0; \quad |\hat{F}| \leq \hat{P} \\ \text{Separation} \quad \hat{F} = 0; \quad \hat{P} < 0 \\ \text{Forward slip} \quad \hat{v} > 0; \quad \hat{P} \geq 0; \quad \hat{F} = -\hat{P} \\ \text{Backward slip} \quad \hat{v} < 0; \quad \hat{P} \geq 0; \quad \hat{F} = \hat{P} \end{array} \right\}, \quad (8)$$

with

$$\hat{P} = 1 + \hat{P}_1 \sin(\omega t); \quad \hat{Q} = \hat{Q}_1 \sin(\omega t + \phi) \quad (9)$$

and

$$\hat{F} = \hat{Q}_1(1 + \hat{v}) \quad (10)$$

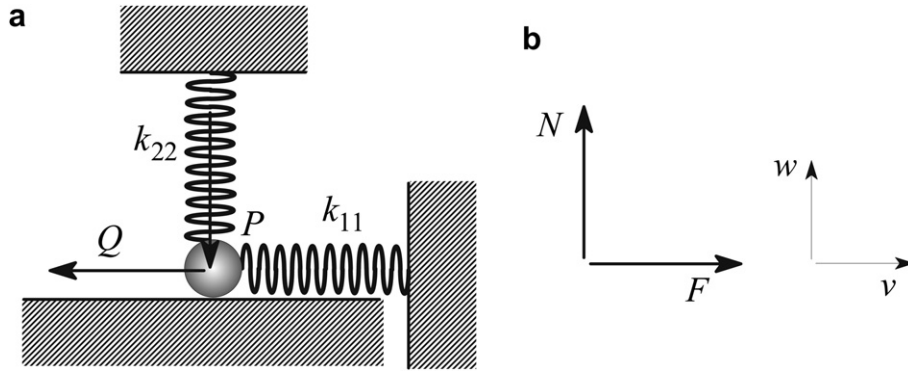


Fig. 2. (a) Single-node frictional system, (b) sign convention for reactions  $F, N$  and displacements  $v, w$ .

We notice that with this notation, the dissipation depends only on the three dimensionless parameters  $\hat{P}_1, \hat{Q}_1, \phi$ , which will enable us to present a fairly general set of results.

### 2.2. Numerical solution

The numerical solution of these equations and inequalities was performed using a simplified version of the algorithm described by Ahn and Barber (2008). It is tentatively assumed that the state during a given time increment is the same as that in the previous increment, in which case the reactions and displacements at the end of the increment can be calculated from Eq. (8). These results are then checked against the corresponding inequalities and if a violation is detected, a state change is implemented following the scheme outlined in Ahn and Barber (2008). The accuracy of this procedure depends on the use of a sufficiently small time increment to pinpoint these state changes accurately.

## 3. Results

### 3.1. Analytical solution for $\phi = 0$

For the special case where  $\phi = 0$ , an analytical solution can be obtained for the steady state and the resulting values of dissipation are reported by Jang and Barber (2011) as

$$\begin{aligned} \widehat{W} &= 0 & |\hat{P}_1| < 1; |\hat{Q}_1| < 1 \\ &= \frac{4(|\hat{Q}_1|-1)(|\hat{Q}_1|-\hat{P}_1^2)}{(\hat{Q}_1-\hat{P}_1^2)} & |\hat{P}_1| < 1; |\hat{Q}_1| > 1 \end{aligned} \quad (11)$$

$$\begin{aligned} &= 0 & |\hat{P}_1| > 1; |\hat{Q}_1| < |\hat{P}_1| \\ &= \frac{(|\hat{Q}_1|-\hat{P}_1)(1+\hat{P}_1)^2}{|\hat{P}_1|(|\hat{Q}_1|+\hat{P}_1)} & |\hat{P}_1| > 1; |\hat{Q}_1| > |\hat{P}_1|. \end{aligned} \quad (12)$$

The absolute value signs can be removed from  $\hat{P}_1, \hat{Q}_1$  since we chose the coordinate system to ensure that these parameters are positive, but they are left in Eqs. (11) and (12) in the interests of consistency with Jang and Barber (2011). These results were used to validate the numerical algorithm and to explore the effect of the time step on numerical convergence.

Fig. 3 shows a contour plot of the dimensionless dissipation per cycle  $\widehat{W}$  as a function of  $\hat{P}_1, \hat{Q}_1$  for  $\phi = 0$ . Notice that shakedown (Klarbring et al., 2007) occurs if  $\hat{P}_1 < 1$  and  $\hat{Q}_1 < 1$ . In this case, there is no separation and after an initial period of slip, the system reaches a position that lies between the bounds  $|F| < fN$  throughout the cycle and no further slip occurs.

We also notice that no dissipation occurs with  $\phi = 0$  if  $\hat{P}_1 > 1$  and  $\hat{Q}_1 < \hat{P}_1$ . In this case, separation occurs during periods when  $\hat{P} > 1$ , so this state cannot properly be described as shakedown. In fact, this condition is analogous to that in the Mindlin-Deresiewicz problem, where loading and unloading follow the same path and  $dQ/dP < f$  so that there is no tendency to slip at any point in the cycle.

Outside these ranges, dissipation increases monotonically with  $\hat{Q}_1$ , as we might expect, since the amplitude of slip displacement increases with  $\hat{Q}_1$ . However, the dissipation also decreases monotonically with  $\hat{P}_1$ . For this result, notice that an increase in the normal force  $\hat{N}$  increases the frictional force  $\hat{F}$ , whilst reducing the slip amplitude. These effects have opposite effects on the dissipation. However, when  $\hat{P}_1 > 1$ , part of the cycle occurs in separation, during which no dissipation occurs.

These limiting conditions provide some background to the numerical results that follow.

### 3.2. Simulation results for $\phi \neq 0$

In Fig. 4, we present similar contour plots of dimensionless dissipation for values of the phase lag  $\phi$  in the range  $0 < \phi < \pi$ . These plots provide an overview of the effect of all three parameters on the frictional dissipation per cycle. Notice that the results repeat in the range  $\pi < \phi < 2\pi$ , such that the dissipation for  $\phi + \pi$  is identical to that for  $\phi$ . In particular, Fig. 3 also applies for  $\phi = \pi$ .

In interpreting these plots, notice that for  $\hat{P}_1 < 1$ , the entire loading cycle involves contact, whereas for  $\hat{P}_1 > 1$ , part occurs in separation, tending to a maximum of 50% of the cycle as  $\hat{P}_1 \rightarrow \infty$ . For clarity, these two régimes are separated by a vertical line at  $\hat{P}_1 = 1$  in Fig. 4.

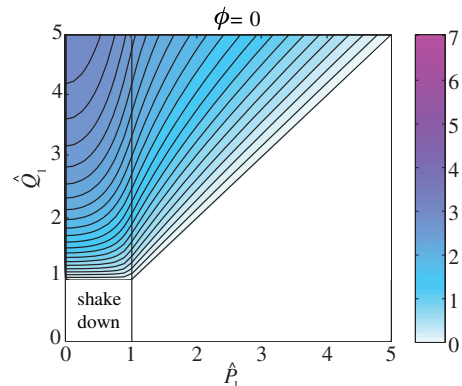


Fig. 3. Contour plot of  $\widehat{W}$  for  $\phi = 0$ . Contact occurs throughout the cycle for  $\hat{P} < 1$  and separation during part of the cycle for  $\hat{P} > 1$ .

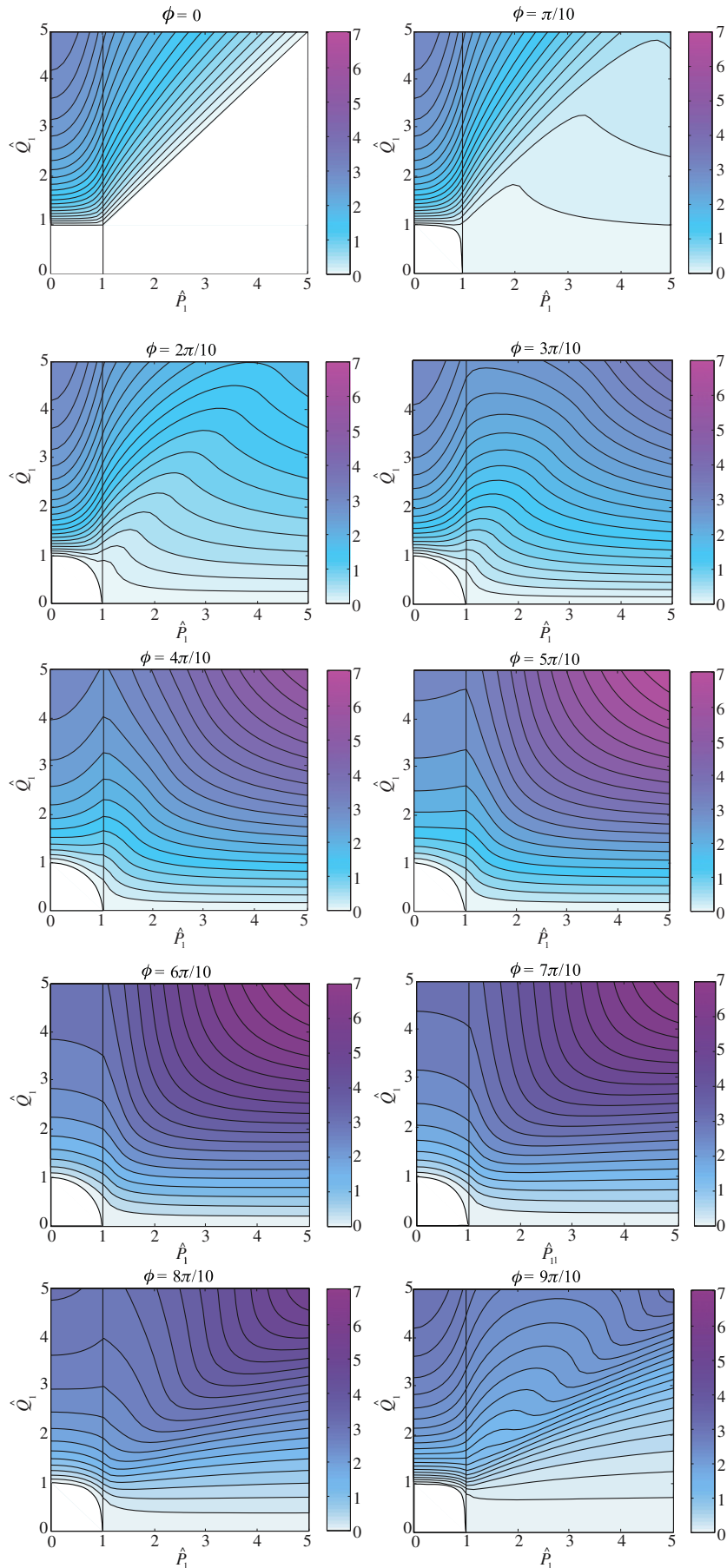


Fig. 4. Contour plots of  $\widehat{W}$  for various values of  $\phi$ .

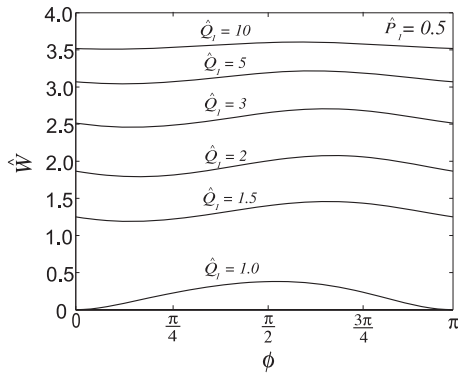


Fig. 5. Dimensionless dissipation  $\widehat{W}$  as a function of  $\phi$  for  $\widehat{P}_1 = 0.5$  (in the full contact régime) and various values of  $\widehat{Q}_1$ .

In the full contact régime  $\widehat{P}_1 < 1$ , the phase has a comparatively small effect on dissipation, except when  $\widehat{Q}_1$  is small. For example, Fig. 5 shows dissipation as a function of  $\phi$  for  $\widehat{P}_1 = 0.5$  and various values of  $\widehat{Q}_1$ . It follows that a reasonable estimate of the dissipation can be obtained from equation (11), which is of course exact for  $\phi = 0$ .

For all values of  $\phi$ , the contour plots of Fig. 4 exhibit a region of shakedown (zero dissipation) near the origin. This corresponds to the condition in which there exists a shift in the  $Q$ -direction that would move the ellipse of Fig. 1 to a location completely within the range between the lines  $Q = \pm P$ . This shift corresponds to a constant (time-invariant) slip displacement  $\nu$  in Eq. (2).

Some separation must occur during the cycle if  $\widehat{P}_1 > 1$  and in this régime, the contour plots of Fig. 4 show a region of high dissipation developing as  $\phi$  is increased from zero (of course the dissipation occurs during the contact phase of this cycle). This effect reaches a maximum near  $\phi = 0.6\pi$  and then falls back to zero as  $\phi$  approaches  $\pi$ . It is highlighted in Fig. 6 which presents the dimensionless dissipation as a function of  $\phi$  for  $\widehat{P}_1 = \widehat{Q}_1 = 5$ . Notice that the curve is not symmetrical and the maximum occurs at  $\phi = 0.6\pi$ . The curves in the contour plot for  $\phi = 6\pi/10$  are approximately hyperbolic for large  $\widehat{P}_1, \widehat{Q}_1$  and the corresponding values of dissipation in this region are approximately given by  $\widehat{W} \approx 1.6\sqrt{\widehat{P}_1\widehat{Q}_1}$ .

The phase lag at which the maximum dissipation occurs varies somewhat with the loading parameters. For example, Fig. 7 shows the dissipation as a function of  $\phi$  for  $\widehat{P}_1 = 1.5$  and various values of  $\widehat{Q}_1$ . The maximum dissipation occurs at  $\phi = \pi/2$  when  $\widehat{Q}_1$  is small and large compared with unity, but is displaced to the right for intermediate values. Notice also that the phase lag has a quite

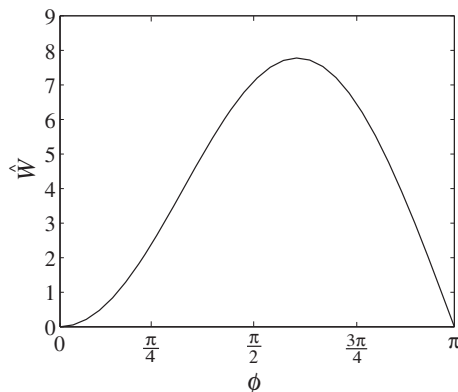


Fig. 6. Dimensionless dissipation  $\widehat{W}$  as a function of  $\phi$  for  $\widehat{P}_1 = \widehat{Q}_1 = 5$ .

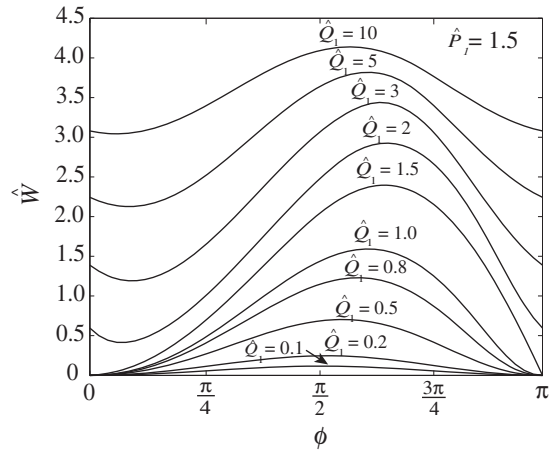


Fig. 7. Dimensionless dissipation  $\widehat{W}$  as a function of  $\phi$  for  $\widehat{P}_1 = 1.5$  and several values of  $\widehat{Q}_1$ .

significant effect on dissipation even though the separation period accounts for only 17% of the loading cycle for this value of  $\widehat{P}_1$ .

### 3.3. An example

The dimensionless notation of Eq. (6) enables us to present the results in the most general possible form, but might present a barrier to comprehension of the physical behavior of typical systems. We therefore here present results for a simple example, comprising a motor bolted to a foundation, as shown in Fig. 8. We suppose that the rotor has a mass  $M$  whose center of mass is displaced by a small distance  $\delta$  from the axis of rotation, which tends to cause a harmonic vibration when the rotor rotates at constant speed  $\Omega$ . The bolts are tightened so as to give a compressive contact force  $P_0$  when the rotor is stationary, so that during operation the loading on the bolted joint will be of the form (1) with  $P_1 = Q_1 = M\Omega^2\delta$ ,  $\omega = \Omega$  and  $\phi = \pi/2$ . It follows that,

$$\widehat{P}_1 = \frac{M\Omega^2\delta}{P_0}; \quad \widehat{Q}_1 = \frac{M\Omega^2\delta}{fP_0}$$

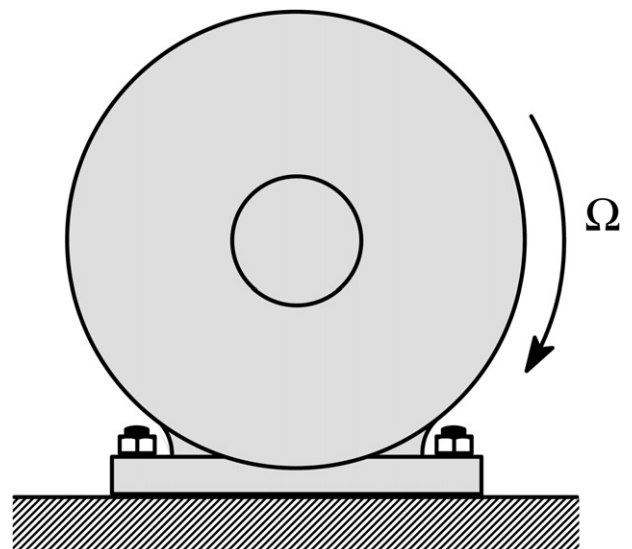


Fig. 8. Motor bolted to a foundation.

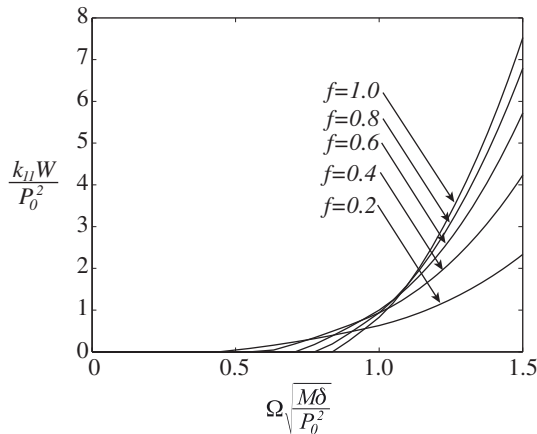


Fig. 9. Dissipation as a function of rotational speed for several values of the coefficient of friction  $f$ .

and in particular,  $\hat{Q}_1 = \hat{P}_1/f$  which corresponds to a straight line of slope  $1/f$  on the contour plot for  $\phi = 5\pi/10$  in Fig. 4.

Fig. 9 shows the resulting dissipation as a function of rotational speed for various values of the coefficient of friction. The stiffness component  $k_{11}$  can be regarded as a measure of the tangential stiffness of the bolted joint. Studies of the contact of rough surfaces suggest that this is of the same order as the corresponding normal stiffness and increases with the preload approximately with  $P_0/\gamma\sigma$  where  $\sigma$  is a measure of the combined height distribution of the contacting surfaces and  $\gamma$  is a dimensionless parameter of order unity (Akarapu et al. 2010).

The analysis given here is restricted to the case where the motion can be regarded as quasi-static and hence where  $\Omega \ll \Omega_0$ , where  $\Omega_0 = \sqrt{k_{11}/M}$  is the natural frequency of tangential vibrations. Using the above estimate for  $k_{11}$ , this implies that the horizontal axis in Fig. 9 corresponds to,

$$\Omega \sqrt{\frac{M\delta}{P_0}} \sim \frac{\Omega}{\Omega_0} \sqrt{\frac{\delta}{\gamma\sigma}}$$

The results from this analysis could be used in an approximate (e.g. harmonic balance) sense at higher rotational speeds, but

would then require iteration between the solution of the underlying dynamics problem including linear damping, with a solution of the quasi-static frictional problem to estimate the effective damping coefficient under the estimated contact loads.

#### 4. Conclusions

This investigation shows that when a simple frictional contact system is subjected to periodic loading, the energy dissipated in friction, and hence the effective damping of the contact, is significantly affected by the relative phase of the fluctuation in normal and tangential loads and is greatest when these are approximately  $\pi/2$  out of phase. The effects are most significant when some separation occurs during the cycle. For a more complex system such as a finite element model of a continuous contact problem, there will always be some nodes that experience periods of separation when the contact is non-conforming (as in the Hertzian problem) as long as the loading scenarios is one in which the normal contact force varies during the cycle.

#### References

- Ahn, Y.J., Barber, J.R., 2008. Response of frictional receding contact problems to cyclic loading. *Int. J. Mech. Sci.* 50, 1519–1525.
- Akarapu, S., Sharp, T., Robbins, M.O., 2010. Stiffness of Contacts between Rough Surfaces. <http://arxiv.org/abs/1011.1479>.
- Barber J. R., Frictional systems subjected to oscillating loads. *Ann. Solid Struct. Mech.* (under review).
- Cattaneo, C., 1938. Sul contatto di due corpi elastici:distribuzione locale degli sforzi, vol. 27. *Rendiconti dell'Accademia Nazionale dei Lincei*, pp. 342–348, pp. 434–436, pp. 474–478. (in Italian).
- Ciavarella, M., 1998. The generalized Cattaneo partial slip plane contact problem: I-theory, II-examples. *Int. J. Solid. Struct.* 35, 2349–2378.
- Jäger, J., 1998. A new principle in contact mechanics. *ASME J. Tribol.* 120, 677–684.
- Jang, Y.H., Barber, J.R., 2011. Frictional energy dissipation in materials containing cracks. *J. Mech. Phys. Solid.* 59, 583–594.
- Klarbring, A., 1990. Examples of non-uniqueness and non-existence of solutions to quasi-static contact problems with friction. *Ing-Arch.* 60, 529–541.
- Klarbring, A., Ciavarella, M., Barber, J.R., 2007. Shakedown in elastic contact problems with Coulomb friction. *Int. J. Solid Struct.* 44, 8355–8365.
- Mindlin, R.D., 1949. Compliance of elastic bodies in contact. *ASME J. Appl. Mech.* 16, 259–268.
- Mindlin, R.D., Deresiewicz, H., 1953. Elastic spheres in contact under varying oblique forces. *ASME J. Appl. Mech.* 75, 327–344.
- Nowell, D., Dini, D., Hills, D.A., 2006. Recent developments in the understanding of fretting fatigue. *Eng. Fract. Mech.* 73, 207–222.